WILEY

Edited by
John K. Gibson and Wibe A. de Jong

Experimental and Theoretical Approaches to Actinide Chemistry

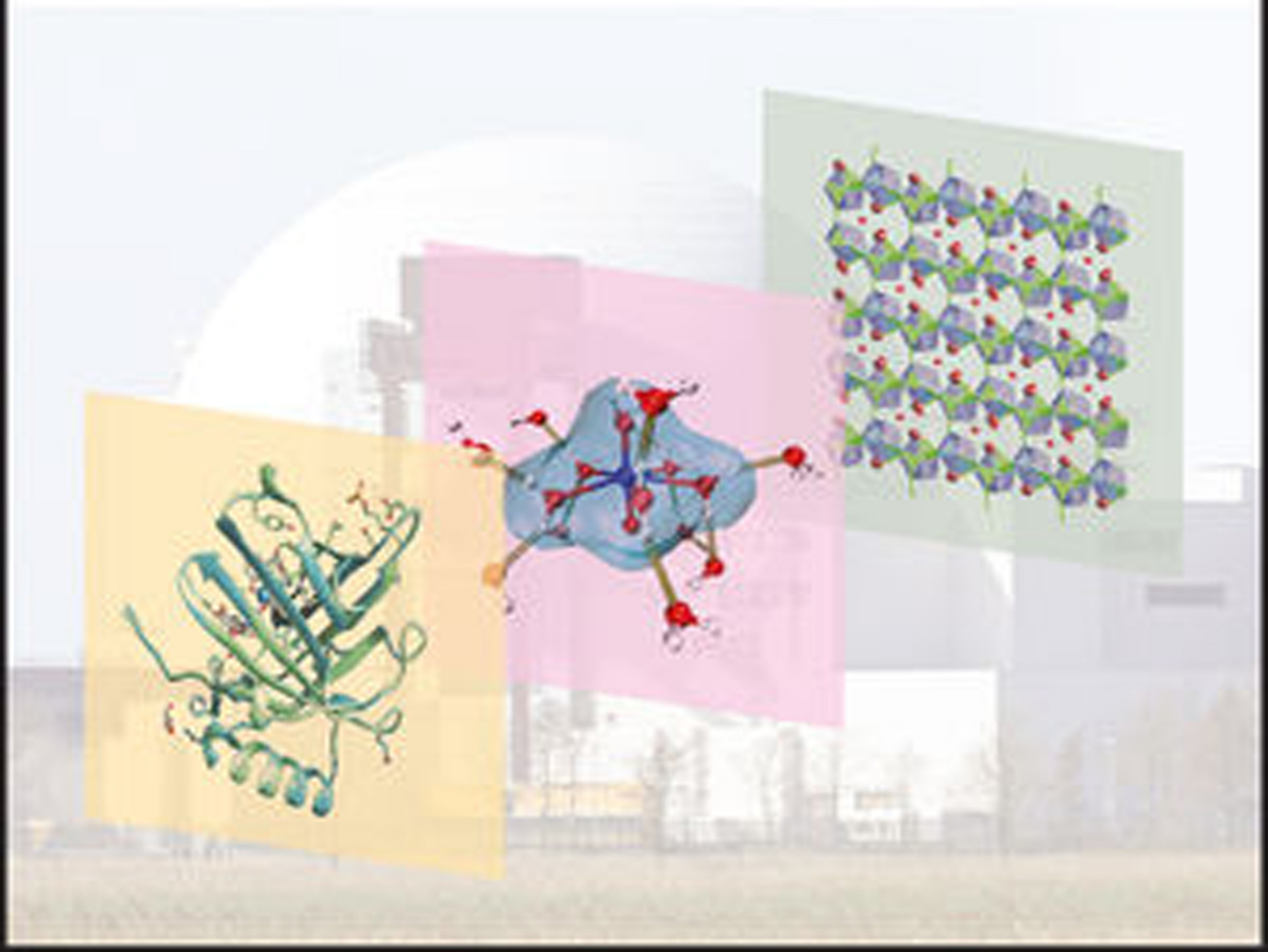

Experimental and Theoretical Approaches to Actinide Chemistry

Experimental and Theoretical Approaches to Actinide Chemistry

Edited by John K. Gibson and Wibe A. de Jong

Lawrence Berkeley National Laboratory
California, United States

WILEY

This edition first published 2018

Registered Office(s)
John Wiley & Sons, Inc., 111 River Street, Hoboken, NJ 07030, USA
John Wiley & Sons Ltd, The Atrium, Southern Gate, Chichester, West Sussex, PO19 8SQ, UK

Editorial Office
9600 Garsington Road, Oxford, OX4 2DQ, UK

For details of our global editorial offices, customer services, and more information about Wiley products visit us at www.wiley.com.

Wiley also publishes its books in a variety of electronic formats and by print-on-demand. Some content that appears in standard print versions of this book may not be available in other formats.

Library of Congress Cataloging-in-Publication Data

Names: Gibson, John K. (John Knight), editor. | Jong, Wibe A. de, 1969– editor.
Title: Experimental and theoretical approaches to actinide chemistry / edited by John K. Gibson (Lawrence Berkeley National Laboratory, CA, USA), Wibe A. de Jong (Lawrence Berkeley National Laboratory, CA, USA).
Description: Hoboken, NJ : Wiley, 2018. | Includes bibliographical references and index. |
Identifiers: LCCN 2017041633 (print) | LCCN 2017052767 (ebook) | ISBN 9781119115533 (pdf) | ISBN 9781119115540 (epub) | ISBN 9781119115526 (cloth : alk. paper)
Subjects: LCSH: Actinium compounds. | Actinide elements. | Heavy elements.
Classification: LCC QD181.A2 (ebook) | LCC QD181.A2 E95 2018 (print) | DDC 546/.421–dc23
LC record available at https://lccn.loc.gov/2017041633

Cover Design: Wiley
Cover Images: Background Image ©Arco Images GmbH/Alamy Stock Photo; Left Image Courtesy of W. A. de Jong (LBNL); Middle Image Courtesy of R. Abergel(LBNL); Right Image Courtesy of Prof. T. Albrecht-Schmitt (Florida State University)

Set in 10/12pt Warnock by SPi Global, Pondicherry, India

10 9 8 7 6 5 4 3 2 1

Contents

List of Contributors

Rebecca J. Abergel
Chemical Sciences Division
Lawrence Berkeley National Laboratory
California
United States

Peter Agbo
Chemical Sciences Division
Lawrence Berkeley National Laboratory
California
United States

Thomas E. Albrecht-Schmitt
Florida State University
Tallahassee, United States

Rami J. Batrice
Department of Chemistry
Georgetown University, Washington, DC
United States

Marjorie Bertolus
CEA, DEN
Centre de Cadarache, France

N. Bryan
National Nuclear Laboratory
United Kingdom

Aurora E. Clark
Department of Chemistry
Washington State University
United States

M.A. Denecke
The University of Manchester
United Kingdom

Trevor W. Hayton
Department of Chemistry and
Biochemistry
University of California Santa Barbara
United States

Michael C. Heaven
Department of Chemistry
Emory University, Atlanta
United States

S. Kalmykov
Lomonosov Moscow State University
Department of Chemistry – Radiochemistry
Russia

Nikolas Kaltsoyannis
School of Chemistry
The University of Manchester
United Kingdom

Karah E. Knope
Department of Chemistry
Georgetown University, Washington, DC
United States

Rudy Konings
European Commission
Joint Research Centre
Karlsruhe
Germany

Gregory R. Lumpkin
Nuclear Fuel Cycle Research
Australian Nuclear Science and
Technology Organisation
New South Wales, Australia

Matthew L. Marsh
Florida State University
Tallahassee
United States

K. Morris
The University of Manchester
United Kingdom

Kirk A. Peterson
Department of Chemistry
Washington State University
United States

F. Quinto
Karlsruhe Institute of Technology
Institute for Nuclear Waste Disposal
Germany

Julian A. Rees
Chemical Sciences Division
Lawrence Berkeley National Laboratory
California
United States

Jenifer C. Shafer
Department of Chemistry
Colorado School of Mines
United States

Jennifer N. Wacker
Department of Chemistry
Georgetown University
Washington, DC
United States

Ping Yang
Theoretical Division
Los Alamos National Laboratory
United States

Preface

This book delivers a contemporary overview of experimental and computational techniques to probe the chemistry and physics of actinides needed for predicting the fate and controlling the behavior of actinide-containing materials in the ecosystem, as well as for developing new advanced applications in energy, medicine, and forensics.

The actinides are located at the bottom of the periodic table, and comprise the 15 elements actinium (Ac; Z = 89) through lawrencium (Lr; Z = 103). Placement of the actinides in the periodic table as a homologous series to the lanthanides was proposed in 1944 by Glenn Seaborg when only a few members of the series had yet been discovered. Seaborg accurately hypothesized that the actinides are characterized by filling of the 5f orbital shell, in analogy with filling of the lanthanide 4f orbital shell. The extensive hexavalent chemistry of U had already been established in 1944, this in stark contrast to the dominant trivalent oxidation state of the lanthanides. The substantially more complex, and interesting, chemistry of the 5f actinides continued to develop with stable oxidation states from II to VII having been characterized.

Some of the early actinides find their use primarily in commercial nuclear reactors, and secondarily in nuclear weapons. Worldwide there is substantial interest in the development of new nuclear reactors with advanced fuel cycles, utilizing a wider range of actinides, with the appropriate safety and nonproliferation constraints to meet the energy needs. In addition, there are ongoing critical issues with respect to the environmental cleanup at production sites of nuclear materials, and storage and reprocessing sites for spent reactor fuels. Understanding the chemistry of the actinides is key to the development of next-generation nuclear reactors, novel actinide reprocessing, and recycling technologies, and to safeguard society against radiological contamination. Research on actinides ranges from the fundamental aspects of actinide bonding to the chemistry and stability of actinide complexes in harsh conditions. The challenges of studying actinides are profoundly complex, as they are hazardous and difficult due to radioactivity, they generally reside in harsh environments, and only small quantities of most actinides are available for research. In the last decade, computational chemistry and materials science has provided another avenue to probe the complex actinide chemistry.

This book is divided into nine chapters and attempts to cover the diversity of actinide chemistry. The chapters focus on the multidisciplinary and multimodal nature of actinide chemistry, the interplay between multiple experiments and theory, as well as between basic and applied actinide chemistry. In covering the central aspects of actinide chemistry, the chapters in this book hopefully will provide a much-needed

reference work for both researchers entering the field of actinide chemistry and those desirous of introducing new techniques into their current actinide research.

Beginning with the most elementary of species, in Chapter 1 Heaven and Peterson provide an overview of the gas-phase chemistry of small actinide-containing molecules. In Chapter 2, Batrice, Wacker, and Knope focus on the speciation and chemistry of actinide species in solution environments. Marsh and Albrecht-Schmitt discuss the world of inorganic actinide materials, covering a large number of known actinide structures, in Chapter 3. In Chapter 4, Hayton and Kaltsoyannis provide an experimental and computational overview of organometallic actinide complexes with novel oxidation states and ligand types. The remaining five chapters are focused on the various natural and engineering environments where actinides are being encountered. The chemistry behind solvation extraction used in separation processes are discussed in Chapter 5 by Clark, Yang, and Shafer. Konings and Bertolus provide a detailed overview of the behavior and properties of the complex nuclear reactor fuel materials in Chapter 6. Lumpkin discusses nuclear waste forms and the effects of radiation damage in Chapter 7. In Chapter 8, Denecke, Bryan, Kalmykov, Morris, and Quinto present an overview of actinide sources and their behavior and mobility in natural environments. Finally, in Chapter 9, Agbo, Rees, and Abergel gives an overview of actinides in biological systems.

We would like to thank all authors of the chapters for their hard work, outstanding contributions, and patience as we brought all the chapters together. Your work is greatly appreciated. We would like to thank Teresa Eaton for her help in copyediting the manuscript.

1

Probing Actinide Bonds in the Gas Phase: Theory and Spectroscopy

Michael C. Heaven[1] *and Kirk A. Peterson*[2]

[1] *Department of Chemistry, Emory University, Atlanta, Georgia, United States*
[2] *Department of Chemistry, Washington State University, Pullman, Washington, United States*

1.1 Introduction

Theoretical studies of actinide compounds have two primary goals. The first is to understand the chemical bonding within these materials and their physical properties. A sub-focus within this task is the elucidation of the roles played by the 5*f* electrons. The second goal is to understand the reactivities of actinide compounds. The long-term objective is to develop reliable computational methods for exploring and predicting actinide chemistry. This is highly desirable owing to the practical difficulties in handling the radioactive and short-lived elements within this family.

Actinides pose a severe challenge for computational quantum chemistry models due to the large numbers of electrons and the presence of strong relativistic effects [1–4]. Although small molecules (di- and tri- atomics that contain just one metal atom) can be explored using rigorous theoretical models, the computational cost of this approach is currently too high for most problems of practical interest (e.g., actinide ions interacting with chelating ligands in solution). Consequently, approximate methods are applied. Ab initio calculations can be accelerated by using a single effective core potential to represent the deeply bound electrons of the metal atom [5, 6]. The relativistic effects are folded into this core potential, and the number of electrons explicitly considered by the calculations is greatly reduced. Semi-empirical density functional theory (DFT) methods offer even better computational efficiency. It is, of course, essential that these approximate methods be tested against both accurate experimental data and the results of rigorous "benchmark" calculations.

There are clear advantages for using data obtained from gas-phase measurements for the comparisons with theory. The ideal situation is to evaluate predictions for the bare molecule against experimental data that are untainted by interactions with solvent molecules or a host lattice. Gas-phase spectroscopy can provide accurate determinations of rotational constants, dipole moments, vibrational frequencies, electronic excitation energies, ionization energies, and electron affinities [7–11]. Information concerning the geometric structure and the electronic state symmetries can be derived from the

Experimental and Theoretical Approaches to Actinide Chemistry, First Edition.
Edited by John K. Gibson and Wibe A. de Jong.

rotational energy level patterns, which can only be observed for the unperturbed molecule. The reactivities of actinide-containing species can also be investigated in the gas phase, under conditions that facilitate theoretical comparisons [8, 12–15]. The majority of this work relies on mass spectrometry for the selection of the reactants and identification of the products. In addition to revealing reaction pathways, mass spectrometric experiments provide critical thermodynamic data, such as bond dissociation and ionization energies.

Over the past 30 years, there has been steady progress in the development of relativistic quantum chemistry methods, combined with a dramatic increase in the speed and capacity of computing platforms. On the experimental side, the application of laser-based spectroscopy, guided ion beam, and ion-trap mass spectrometry has significantly advanced our ability to explore the structure, bonding, and reactivity of actinide species. In this chapter, we present an overview of the theoretical and experimental techniques that are currently being used to gain a deeper understanding of actinides through the studies of small molecules in the gas phase. While some background material is presented, the primary focus is on the techniques that are currently being applied and developed. To limit the scope, the experimental section is strictly devoted to gas-phase measurements. There is a large body of excellent spectroscopic work that has been carried out for actinide species trapped in cryogenic rare-gas matrices. The data from these measurements are also of great value for tests of theoretical predictions, as the rare-gas solid is usually a minimally perturbing host. For a review of the matrix work, see Reference [8]

1.2 Techniques for Obtaining Actinide-Containing Molecules in the Gas Phase

The earliest spectroscopic studies of actinide-containing molecules in the gas phase were carried out using compounds that possessed appreciable vapor pressures at room temperature. Hence, the hexafluorides UF_6, NpF_6 and PuF_6 were studied by conventional spectroscopic means [8], with suitable precautions for handling radionuclides. The tetrahalides have lower room temperature vapor pressures, but workable number densities have been obtained using moderate heating of the samples [8]. Studies of thorium oxide (ThO) emission spectra were carried out using ThI_4 as the source of the metal [16]. This reagent was subjected to a 2.45 GHz microwave discharge that was sustained in approximately 0.1 Torr of Ne buffer gas. The oxide was readily formed by the reaction of the discharge-generated Th atoms with the walls of the quartz tube that contained the ThI_4/Ne mixture. Molecular ions can also be generated at workable number densities using discharges with volatile compounds. An example is provided by the recent study of ThF^+ reported by Gresh et al. [17]. ThF_4 was used as the starting reagent, and the vapor pressure was increased by heating the quartz discharge tube to 1193 K. The tube was filled with approximately 5 Torr of He, and the mixture was excited by an AC discharge operated at a frequency of 10 kHz.

More commonly, actinide species are refractory solids that require somewhat extreme conditions for vaporization. Tube furnaces [18, 19], Knudsen ovens [20, 21], discharge sputtering [14], discharges [16, 17, 22], and laser ablation techniques [8, 23–25] have been successfully applied. High-temperature vaporization is exemplified by

studies of the electronic spectrum of uranium oxide (UO), carried out using a Knudsen oven to vaporize U-metal samples that had been pre-oxidized by exposure to air [21]. The crucible was heated to temperatures in the range of 2400–2600 K. This was high enough that thermally excited electronic transitions could be observed using conventional emission spectroscopy. The UO vapor pressure generated by the Knudsen oven was sufficient for the recording of absorption and laser-induced fluorescence (LIF) spectra. Resistively heated tube furnaces have also been used for studies of gas-phase UO. The advantage of this approach is that it provides a longer optical path length, and thereby yields spectra with greater signal-to-noise ratios. Extensive high-resolution electronic spectra for UO were recorded by Kaledin et al. [18] using a tube furnace that was heated to 2400 K. More recently, Holt et al. [19] have used a tube furnace to record microwave absorption spectra for UO in the 500–650 GHz range. Transitions between the rotational levels of multiple low-lying electronic states (including the ground state) were observed.

Many of the early mass spectrometric studies of gas-phase actinide molecules were carried out using thermal vaporization in combination with electron impact ionization techniques [26–28]. Surface ionization of uranyl acetate has been used to generate UO^+ and UO_2^+ [29]. In the thorium ion experiments of Armentrout et al. [14, 30], thorium powder was mounted in a cathode held at −2.5 kV. This electrode produced a discharge in a flow of Ar, and the resulting Ar^+ ions generated Th^+ by sputtering. Molecular ions, such as $ThCH_4^+$, were formed in a downstream flow tube. These techniques are suitable for measurements that rely on charged particle detection, but the number densities are usually too small for conventional spectroscopic observations (e.g., absorption or fluorescence detection).

For spectroscopic techniques that are compatible with pulsed generation of the target species, laser vaporization has proved to be a particularly versatile method. The products include cations, anions, and molecules in exotic oxidation states. Duncan [23] has published a very informative review of this technique. Typically, a pulsed laser (Nd/YAG or excimer with 5–10 ns pulse duration) is focused onto the surface of a target to produce a vapor plume. The products are cooled and transported using a flow of an inert carrier gas (e.g., He or Ar). If the plume does not contain the species of interest, the carrier gas can be seeded with a reagent that will produce the desired product. For example, gas-phase UF has been produced by vaporizing U metal into a flowing mixture of He and SF_6 [31].

Charged species are produced by the vaporization process, even in the absence of an externally applied electric field. Cations are formed by thermal processes and photoionization. Some of the liberated electrons attach to neutral molecules, providing a viable flux of negative ions under suitable conditions. External fields can be applied if the initial ion yield is not high enough for the detection technique.

A particularly valuable advantage of the laser vaporization technique is that it can be readily combined with a supersonic jet expansion nozzle. Figure 1.1 (reproduced from Reference [23]) shows this combination for a pulsed solenoid gas valve (labeled "General Valve"). The valve supplies a high-pressure pulse of carrier gas, timed to coincide with the laser vaporization pulse. The entrained plume passes through a reaction channel before expansion into a vacuum chamber. On expansion, the gas temperature and density drops rapidly. The internal degrees of freedom for entrained molecules can be relaxed to population distribution temperatures in the range of 5–20 K. Condensation

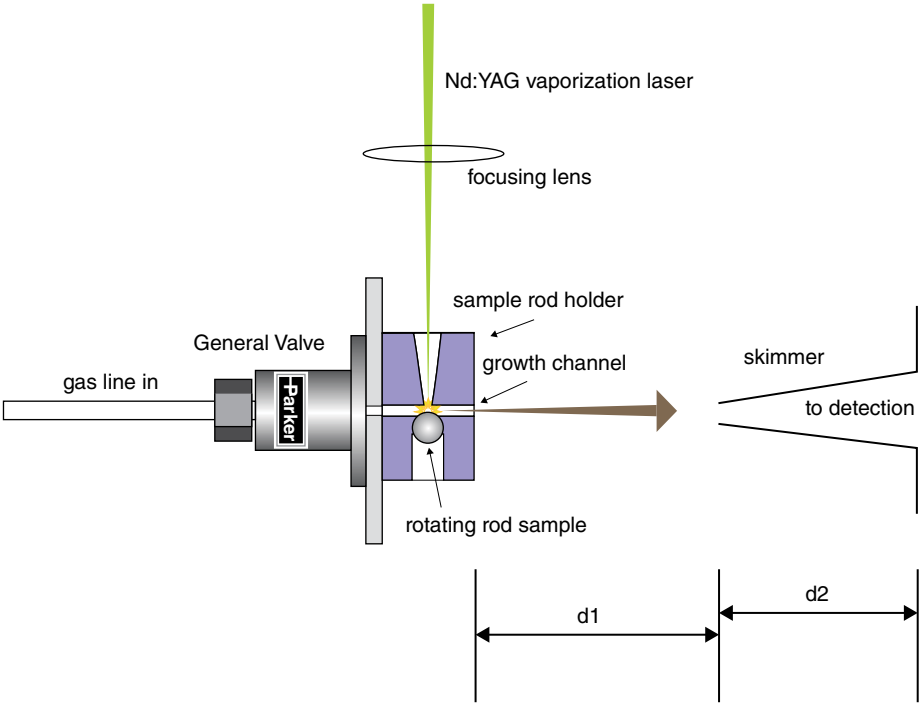

Figure 1.1 The general schematic design of a "standard" laser vaporization cluster source (Reproduced with permission from Duncan, M.A. (2012) Invited review article: Laser vaporization cluster sources. *Review of Scientific Instruments*, **83**, 041101/1–041101/19.)

is prevented by the concomitant drop in gas density. The cooling greatly facilitates spectroscopic studies by dramatically reducing the number of thermally populated internal energy states. In this context, it is useful to note that the rapid expansion often leads to non-equilibrium population distributions. Collisional relaxation rates are sensitive to the energy spacings between levels, and they are most favorable for the smallest energy intervals (provided that there are no symmetry restrictions involved). Transfer between the closely spaced rotational levels is facile. Consequently, low rotational temperatures are easily attained. The more widely spaced vibrational levels require a larger number of collisions for effective relaxation. As the number of collisions is limited by the expansion kinetics, the final population distribution will often show a vibrational temperature that is substantially higher than the rotational temperature. Lastly, the pulsed vaporization process can populate metastable electronically excited states, which can be quite resistive to cooling in the expansion. A study of the jet-cooled Be_2 dimer illustrates this hierarchy [32]. The rotational temperature was 7 K, the vibrational temperature was near 160 K, and an electronically excited triplet state with an energy of 7406 cm^{-1} was substantially populated.

The gas dynamics can also be used to exert some control over the chemistry occurring in the expansion. One way this can be accomplished is by varying the length of the "growth channel" as shown in Figure 1.1. Lengthening this channel increases the time for which the density of reactive species is high enough for chemistry to occur. As a

simple example, clusters of metal atoms are often seen following vaporization of a metal target. The mean size of the clusters increases with the length of the growth channel. There are several other factors that influence the chemistry. These include the concentrations of reactants added to the carrier gas, the laser power, wavelength, and pulse duration. Duncan [23] provides a helpful discussion of the effects of these parameters.

Electrospray ionization (ESI) provides a versatile means of producing both cations and anions in the gas phase [33]. ESI is a soft ionization method that can produce complex ions that would not survive the harsh conditions of thermal vaporization or laser ablation. Multiply charged ions can be made, along with partially solvated species that yield insights concerning solution phase speciation. For this technique, actinide salts are first dissolved in a polar solvent (e.g., water, methanol, or acetonitrile). The solution is then forced through a metal capillary tube that is held at a high voltage (on the order of a few kilovolts). Ionization and droplet fragmentation occurs as the liquid exits the capillary tube. The products are de-solvated and then sampled into ion traps and/or mass spectrometers. Gibson and coworkers [10, 13, 34–41] have made extensive use of ESI to study reactions of both bare and solvated actinide ions. Gibson's laboratory has the rare capability of handling samples that are radiologically challenging (e.g., Pa, Pu, Am, and Cm). Spectroscopic studies of cations produced by ESI have been performed by means of action spectroscopy, which permits the application of charged particle detection [24, 42–48]. Anions can also be produced by ESI and characterized by photoelectron spectroscopy. Wang [33] has recently reviewed the application of these techniques to actinide-containing anions.

1.3 Techniques for Spectroscopic Characterization of Gas-Phase Actinide Compounds

1.3.1 Conventional Absorption and Emission Spectroscopy

The volatile hexafluorides UF_6, NpF_6, and PuF_6 have been examined using IR and optical absorption spectroscopy [8, 49–55]. Data for these molecules, recorded under room temperature conditions, are complicated by the thermal population of many low-energy ro-vibronic states. For example, it has been estimated that 99.6% of UF_6 molecules populate vibrationally excited levels at 300 K [53, 56]. This problem has been partially mitigated by working with low-temperature cells, but the temperature dependence of the vapor pressure imposes a practical lower limit of about 160 K. Lower temperatures have been achieved for UF_6 using isentropic gas expansion techniques [57, 58]. Due to the large flow rates needed for this technique, it does not appear to have been applied to NpF_6 or PuF_6. Electronic spectra for the hexafluorides have been examined at room temperature, but the level of congestion yields data that are difficult to assign.

Electronic emission spectra for ThO and UO have been recorded using standard monochromators for dispersion. Thermal excitation of UO [21] and discharge excitation of ThO [16, 59–67] yielded emission intensities that were sufficient for the recording of spectra at the Doppler limit of resolution. Rotationally resolved electronic spectra have been obtained over the range from the near-UV to the near-IR. In these studies, the data were recorded by means of photographic plates or high-gain photomultiplier tubes. Owing to the high-temperature source conditions, many levels of the oxides were significantly populated. In the case of UO, Kaledin et al. [21] reported seeing approximately 500 vibronic bands

within the 400–900 nm range. Despite this complexity, several assignable bands were identified. This was possible due to the relatively large rotational constants of the monoxide. Kaledin et al. [21] were also able to record absorption spectra for UO using a continuum light source (Xenon lamp) and a monochromator.

Pure rotational spectroscopy, conducted in the microwave and sub-millimeter wave regions, can provide some of the most accurate molecular constants. At these low transition energies, both the Doppler and lifetime broadenings of the spectral lines are smaller by orders of magnitude, as compared to the visible region. This is conveniently exemplified by UO. For the experiments of Kaledin et al. [21], the Doppler width near 500 nm was 1.3 GHz, and the natural linewidth was approximately 1 MHz. By contrast, the sub-millimeter spectrum of UO, recorded by Holt et al. [19] at a temperature of 2200 K, had a Doppler linewidth of 1.3 MHz, and the natural linewidth was below the effects of pressure broadening. The sub-millimeter wave data for UO were recorded using a frequency modulation technique, and over 280 lines were observed within the 510–652 GHz range. Prior to this study, Cooke and coworkers [68–70] were the first to obtain a microwave spectrum for an actinide-containing molecule (ThO). For these measurements, they used laser ablation and jet expansion cooling to obtain cold gas-phase samples of ThO. A cavity-enhanced absorption technique was used to achieve high sensitivities. Pulsed excitation was used, and the spectra were recovered via Fourier analysis of the time-dependent response. Due to the non-equilibrium nature of jet cooling, they were able to record the pure rotational lines ($J = 0 \rightarrow 1$) for $^{232}Th^{16}O$ vibrational levels ranging from $v = 0$ to 11 (transitions of the $Th^{17}O$ and $Th^{18}O$ isotopes were also examined for lower vibrational levels).

1.3.2 Photoelectron Spectroscopy

Gas-phase photoelectron spectra have been recorded for a small number of Th and U compounds, including UO, UO_2 [71], UF_6 [72], ThX_4, and UX_4 (X = F, Cl, and Br) [73–76]. The vapors were generated by heating solid samples, and the molecules were ionized by means of monochromatic VUV light (e.g., the He II line at 40.8 eV). Ionization energies and spectra for the molecular ions were derived by measuring the kinetic energy distributions of the photoelectrons. This was accomplished using a hemispherical electrostatic analyzer, which is capable of resolving down to about 40 cm^{-1}. This is sufficient to distinguish well-separated vibrational levels and electronically excited states. However, the actinide ions often possess multiple low-lying electronic states, due to the presence of partially filled *d*- or *f*- orbitals on the metal. For molecular ions such as UO^+ and UO_2^+, the low-energy vibrational states are so dense that their photoelectron spectra yield broad, unresolved features [71]. A summary of the gas-phase photoelectron studies of simple actinide compounds is given in Reference [8]. Higher-resolution data for molecular ions have since been obtained using the laser-based methods described in the following sections.

1.3.3 Velocity Modulation and Frequency Comb Spectroscopy

Spectroscopic studies of molecular ions are challenging due to the low densities at which ions can be generated. The concentrations are limited by the reactive nature of the ions, and their Coulombic repulsion. Consequently, ions are nearly always accompanied by

much higher concentrations of neutral molecules. In most instances, the spectra for the neutrals will mask the much weaker signals from the ions. One solution to this problem is to use velocity modulation of the ions [77–79]. This technique requires a tunable laser light source that has a linewidth that is comparable to or smaller than the Doppler linewidth of the transition of interest. Ions are generated in a discharge tube using an alternating current with a frequency in the kilohertz range. During each cycle, the ions are accelerated back and forth along the tube. The laser is propagated along the tube axis, and the transmitted intensity is monitored. If the laser is tuned to the edge of an absorption line, the transmitted intensity will be modulated as the ions are Doppler-tuned in and out of resonance. By observing the signal at the modulation frequency (or multiples thereof), the detection can be strongly biased in favor of the ions (transient neutral species may still be detected due to concentration modulation)[79].

Due to the narrow linewidth required for the velocity modulation technique, scanning for new spectral features is a time-consuming process. A dramatic improvement in the data acquisition rate has recently been achieved by combining velocity modulation with frequency comb spectroscopy (for a detailed review of the frequency comb technique, see Reference [80]). Briefly, a femtosecond pulsed laser with a stabilized optical cavity is used to generate a "comb" of laser frequencies. The frequency spacing of the comb is determined by the cavity round trip time, and the comb contains around 10^5 individual frequencies. This radiation is transmitted through the sample, and dispersed using the combination of a virtually imaged phased array (VIPA) disperser (high resolution) and a diffraction grating (low resolution). By this means, every element of the frequency comb is resolved, and their transmitted intensities are recorded. For the detection of ions, velocity modulation and a multipass optical cavity are employed. Figure 1.2 shows the apparatus used by Gresh et al. [17] to record high-resolution spectra for the ThF^+ ion. Bands that were tentatively assigned to the ThO^+ ion were also present in these spectra. Cossel et al. [22] found that data acquisition with the frequency comb system was about 30 times faster than with conventional velocity modulation spectroscopy. To date, ThF^+ is the only actinide-containing species examined using frequency comb spectroscopy. However, it is evident that a wide range of actinide species (ions and neutrals) could be studied using this powerful tool.

1.3.4 LIF Spectroscopy

LIF spectroscopy of electronic transitions is a versatile method that can achieve high resolution (including methods for overcoming Doppler broadening) [79]. In its simplest form, LIF is performed by tuning a laser through absorption bands and detecting the resulting fluorescence without active selection of the detected wavelengths (usually the optical filter used to block scattered laser light, and the characteristics of the photodetector determine the part of the emission spectrum that is most effectively detected). The result is essentially the absorption spectrum, convoluted with the fluorescence quantum yield for the excited state. Pulsed laser excitation works well, and is readily combined with pulsed laser ablation sources. To illustrate the technique, Figure 1.3 shows the main components of the apparatus at Emory University that is used to study the electronic spectra of actinide-containing molecules. The first vacuum chamber of this instrument houses a laser ablation/jet cooling nozzle source. The beam from a pulsed dye laser crosses the expanding jet a few centimeters downstream from the

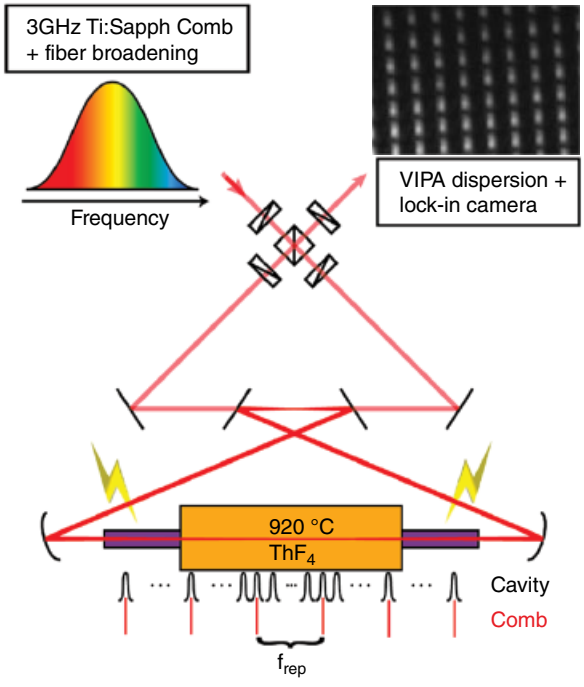

Figure 1.2 The frequency comb/velocity modulation spectrometer. A 3 GHz Ti:Sapphire comb is broadened by a nonlinear fiber and coupled into a bow-tie ring cavity, propagating in either direction through a discharge of ThF_4. Four liquid crystal variable retarders and a polarizing beam splitter control the direction of light propagation through the discharge. After exiting the cavity, the laser light is sent to a cross-dispersive VIPA imaging system with single comb mode resolution and imaged onto a lock-in camera. Approximately 1,500 comb modes are resolved in a single image. (Reproduced with permission from Gresh, D.N., Cossel, K.C., Zhou, Y., Ye, J., and Cornell, E.A. (2016) Broadband velocity modulation spectroscopy of ThF^+ for use in a measurement of the electron electric dipole moment. *Journal of Molecular Spectroscopy*, **319**, 1–9.)

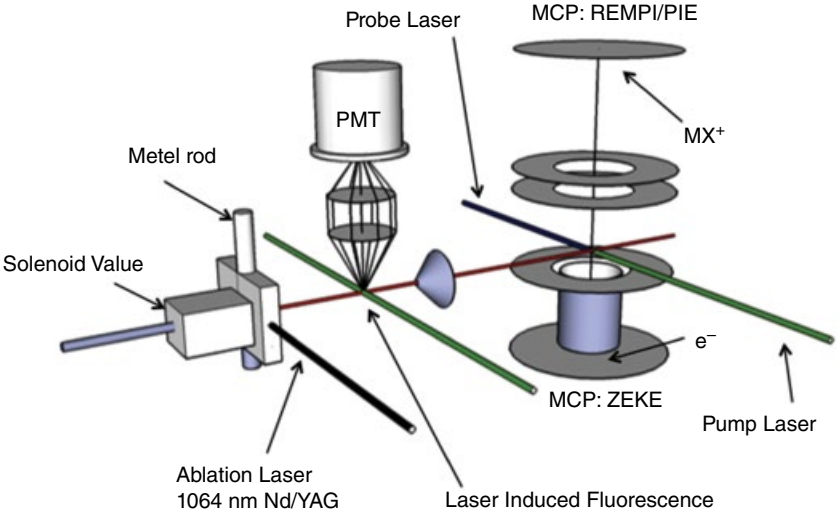

Figure 1.3 Schematic diagram of an apparatus used to record LIF, resonantly enhanced multiphoton ionization (REMPI), PIE, and PFI-ZEKE spectra for gas-phase actinide molecules.

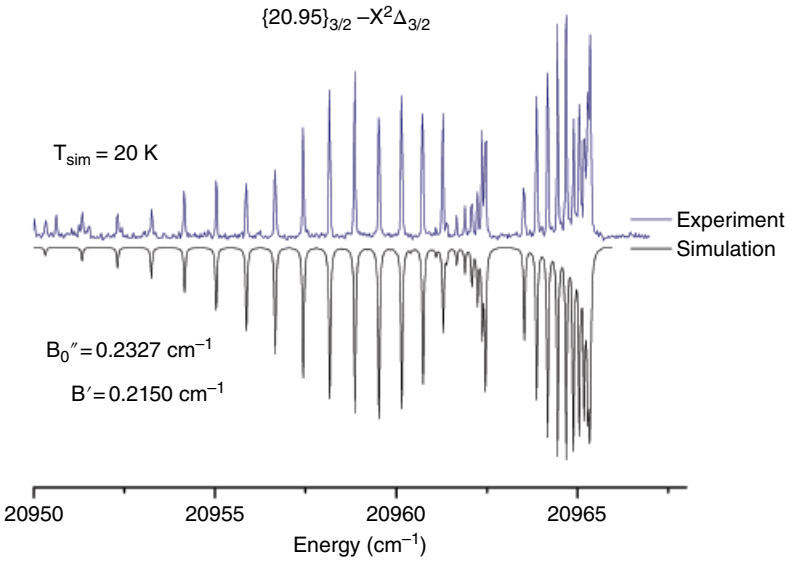

Figure 1.4 Rotationally resolved laser-induced fluorescence (LIF) spectrum of the ThF {20.95}3/2-$X^2\Delta_{3/2}$ band. The downward-going trace is a computer simulation. (*See insert for color representation of the figure.*)

nozzle orifice. The resulting fluorescence is detected along an axis that is perpendicular to the gas flow direction and the probe laser beam. Figure 1.4 shows representative data for ThF. Here, it can be seen that the rotational temperature is low (around 20 K), and the rotational structure is resolved. Note, however, that small splittings associated with breaking of the electronic degeneracy (Ω-doubling) and the hyperfine structure resulting from the nuclear spin of the F atom are not resolved. An advantage of pulsed laser excitation is that the fluorescence can be time-resolved, thereby providing information concerning the lifetimes and transition moments of the excited states.

The resolution of the spectrometer shown in Figure 1.3 is ultimately limited by two constraints. The first is the use of incoherent pulsed laser excitation, which cannot provide a linewidth that is less than that defined by the Fourier transform of the temporal pulse shape. The second limitation is from Doppler broadening. Although the internal temperature within the supersonic flow is low, the molecules are accelerated by the carrier gas as the expansion evolves. If a wide angular spread of the jet is probed by the laser, the supersonic flow velocity (on the order of 1760 ms^{-1} for He) results in appreciable line broadening. This effect can be mitigated by either skimming the core of the expansion into a second vacuum chamber prior to laser excitation, or by masking the fluorescence detection system such that only molecules with low velocities along the laser axis can be observed (a simple slit mask is sufficient). The problem with the laser linewidth can be overcome by switching to a tunable continuous wave (CW) laser. Despite the typically low duty cycle of pulsed laser ablation sources, LIF detection has a high enough sensitivity that the use of a CW probe laser is viable.

The combination of a skimmed molecular beam and a narrow linewidth CW probe laser has been applied to the study of actinide-containing molecules by Steimle and coworkers. To date, this system has been used to examine electronic transitions of ThO

[81], ThS [82], UO [83], and UF [84]. The resolution achieved (around 40 MHz) has been close to the limit imposed by the natural linewidth ($\Delta\nu = \frac{1}{2\pi\tau}$, where τ is the excited state lifetime). This high resolution has permitted measurements of line splitting induced by externally applied electric and magnetic fields. These data yield accurate values for the electric and magnetic dipole moments of both the upper and lower electronic states.

LIF spectra of jet-cooled molecules yield extensive information on electronically excited states, but the data for the ground state may be limited to the properties of the zero-point level. A more extended view of the electronic ground state can be obtained by spectral resolution of the LIF (referred to as dispersed fluorescence in the following text). In addition, the dispersed fluorescence spectra may also reveal the presence of low-energy electronically excited states. Such measurements are particularly effective when the excitation laser is tuned to a single vibronic level of an electronically excited state. The range of ground state vibrational levels observed is dictated by the square of the overlap integral between the upper and lower state vibrational wavefunctions (the Franck–Condon factors). When other electronic states are present, transitions to those that satisfy the usual selection rules are observed. As an example, Figure 1.5 shows a dispersed fluorescence spectrum for ThS, obtained by exciting an upper electronic state with $\Omega = 1$ (where Ω is the unsigned projection of the electronic angular momentum along the bond axis) [85]. The bands on the left-hand side of this spectrum reveal the vibrational structure of the $X^1\Sigma^+$ ground state, while the bands at higher energy are for the $^3\Delta_1$ and $^3\Delta_2$ excited states (the third component of the triplet, $^3\Delta_3$, was not observed as the selection rule is $\Delta\Omega = 0,\pm1$). The range of levels observed in the dispersed fluorescence spectrum can be manipulated, to some extent, through the choice of the initially excited level.

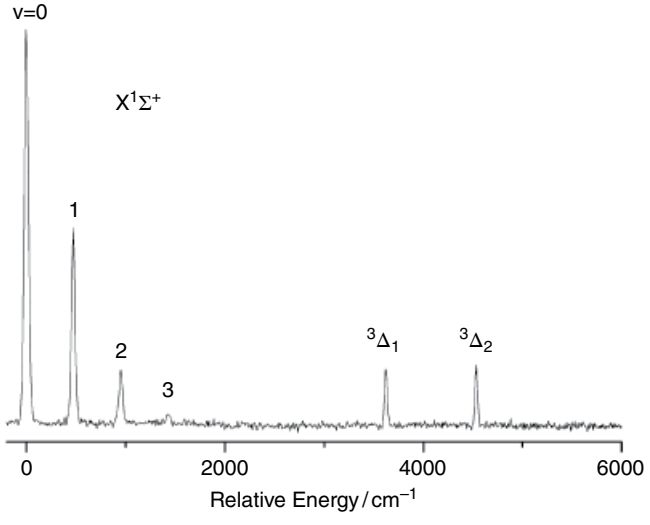

Figure 1.5 Dispersed fluorescence spectrum for ThS recorded using laser excitation of the [22.13]1-$X^1\Sigma^+$ band. (Reproduced with permission from Bartlett, J.H., Antonov, I.O., and Heaven, M.C. (2013) Spectroscopic and Theoretical Investigations of ThS and ThS^+. *Journal of Physical Chemistry A*, **117**, 12042–12048.).

The combination of laser excitation with dispersed fluorescence detection can be used as a two-dimensional method in order to disentangle complex and congested spectra [79]. There are typically two sources of complexity. In laser ablation/jet cooling experiments, the control over the species created is somewhat limited. Consequently, the spectra may include features from several different molecules. The problem is compounded when thermal vaporization or discharge methods are used to obtain gas-phase species. Many states are populated under these conditions, often leading to severe spectral congestion. The dispersed fluorescence technique described earlier, carried out with a fixed excitation wavelength, shows lower state energy levels that are related through their connection to a common upper level. Provided that a sufficiently narrow linewidth is used in excitation, the emission spectrum for a single molecular component of a mixture can be obtained. Once the pattern of low-lying vibronic states has been established, the spectral scanning procedure can be permuted (fix the monochromator, scan the dye laser) or carried out as a coordinated sweep of both the laser and monochromator wavelengths. Spectra recorded with wavelength-selected fluorescence detection (monochromator fixed) show transitions to a specific upper state. This is almost the same information that is obtained using dispersed fluorescence, but restricted to lower levels that are significantly populated. However, a much higher resolution can be achieved via control of the laser linewidth. The excitation spectrum of a specific molecular species, sought under conditions where other species with overlapping spectra are present, can be obtained by a coordinated scan of both the laser and monochromator wavelengths. The tuning rates for both instruments are calculated to keep the energy difference between the absorbed and emitted photons equal to a lower state interval.

An LIF study of the ThF^+ ion illustrates the value of the two-dimensional approach [86]. In these experiments, ThF was generated by laser ablation of Th in the presence of SF_6. Although ThF^+ ions were surely generated by this means, they were not present at a concentration that was sufficient for LIF detection. Additional ThF^+ ions were generated in the downstream region of the jet expansion by means of pulsed laser ionization. The challenge for this experiment was that both ThF and ThF^+ have many overlapping bands in the visible range. ThF dominated the ordinary LIF spectrum, as only a small fraction of the initial ThF was ionized. A further complication was the presence of many intense ThO bands. Metal oxides are nearly always present in laser ablation experiments, and they are very difficult to suppress. Even when high-purity oxygen-free gasses are used, the oxides are routinely observed. The spectrum of ThF^+ was separated from the interfering bands of ThF and ThO by means of the differences in their ground state vibrational intervals ($\Delta G_{1/2}(ThF^+) = 605, \Delta G_{1/2}(ThF) = 653, \Delta G_{1/2}(ThO) = 891\ cm^{-1}$). The clean ThF^+ LIF spectrum shown in Figure 1.6 was obtained with the monochromator set to observe fluorescence that was $605\ cm^{-1}$ red-shifted relative to the excitation energy [86].

So far, we have described the two-dimensional technique as the sequential recording of one-dimensional cuts (fixed laser or fixed monochromator wavelength slices). This strategy is successful, but the rate of data acquisition is slow. In recent years, the technique has been improved by using monochromators equipped with CCD cameras to record the emission spectrum for each point in the laser excitation spectrum (a method that is conveniently combined with pulsed laser excitation). This allows for a more detailed spectral map to be assembled within a reasonable acquisition time. Recent

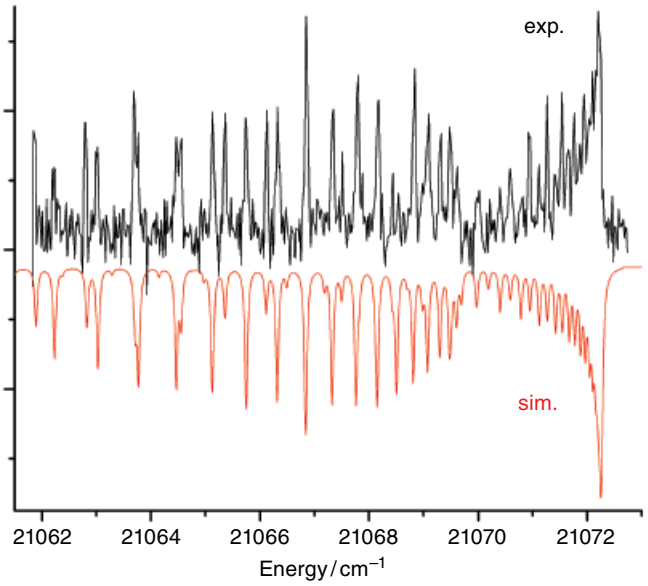

Figure 1.6 Rotationally resolved LIF spectrum of the ThF^+ $[21.1]0^+$-$X^3\Delta_1$ band. The downward-going trace is a computational simulation of the band. (*See insert for color representation of the figure.*)

work by the Steimle group on the first LIF detection of Th_2 illustrates the advantages of this enhancement [87]. The dimer was produced by pulsed laser vaporization of Th metal. As usual, the LIF spectrum, without wavelength selection of the emission, contained many intense bands of ThO. Figure 1.7 shows the two-dimensional spectrum, where a 2000 cm^{-1} segment of the emission spectrum was recorded for every excitation wavelength sampled. Identification of the Th_2 bands in the two-dimensional map is straightforward. Owing to the low vibrational frequency of Th_2, every band of this molecule produces a characteristic column of features. Recording the fluorescence spectrum using the CCD array also facilitates the characterization of relative transition probabilities, as the relative intensities are immune to drifts in the source conditions [88].

1.3.5 Two-Photon Excitation Techniques

The LIF techniques described earlier rely on one-photon excitation processes. With the high intensities provided by lasers and related coherent light sources, there are many two-photon excitation processes that can be exploited. Two-dimensional techniques can be applied if independently tunable light sources are used.

A recent example of a two-photon excitation measurement is the microwave-optical double resonance (MODR) study of ThS reported by Steimle et al. [89]. The MODR technique is a well-established method for recording microwave spectra with a sensitivity that is determined by the electronic transition (electronic transition probabilities are typically orders of magnitude larger than rotational transition probabilities). Figure 1.8 shows the essential components of the MODR experiment. The molecules of interest are entrained in a molecular beam, and a CW laser is used to excite a single rotational line of an electronic transition. The laser beam is divided into two, so that the

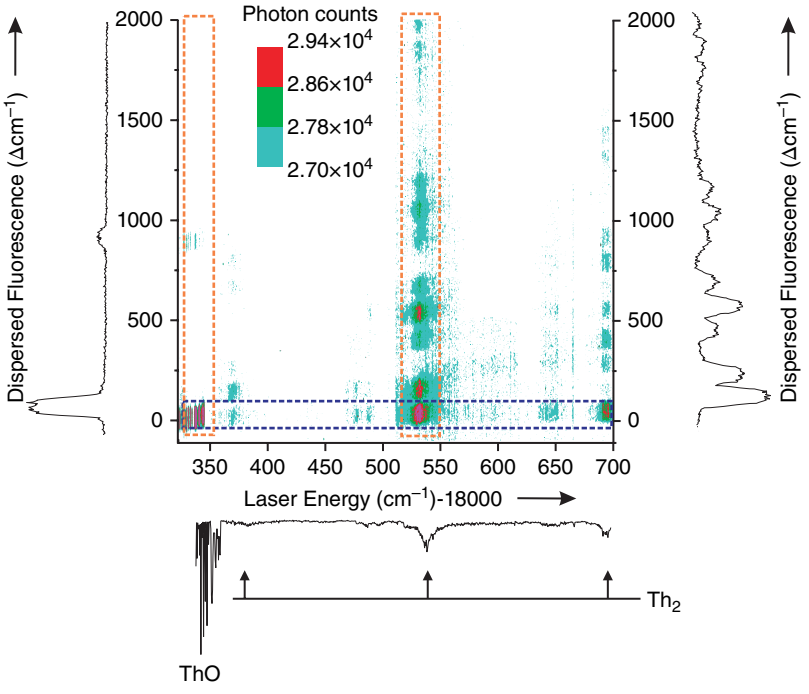

Figure 1.7 2D spectrum over the 18325 – 18700 cm^{-1} laser excitation range of ablated thorium in the presence of a SF6/Ar mixture. Not corrected for laser power variation or the spectral response of the CCD. At the bottom is the on-resonance detected laser excitation spectrum obtained from the vertical integration of the intensities of the horizontal slice marked by the dashed blue rectangle. At the left and right are the dispersed fluorescence spectra resulting from excitation of the (0,0) $F^1\Sigma(+) - X^1\Sigma^+$ band of ThO at 18340 cm^{-1} and Th_2 band at 18530 cm^{-1}, respectively, obtained by horizontal integration of the intensities of the left and right horizontal slices marked in red. (Reproduced with permission from Steimle, T., Kokkin, D.L., Muscarella, S., and Ma, T. (2015) Detection of thorium dimer via two-dimensional fluorescence spectroscopy. *Journal of Physical Chemistry A*, **119**, 9281–9285.) (*See insert for color representation of the figure.*)

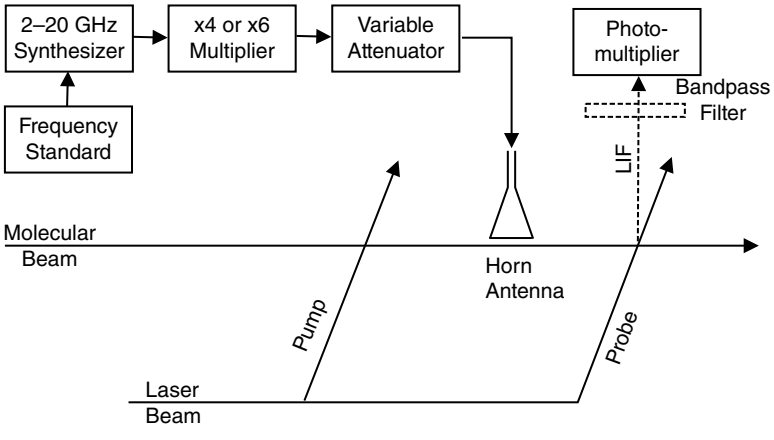

Figure 1.8 A block diagram of the MODR spectrometer. (Reproduced with permission from Steimle, T.C., Zhang, R., and Heaven, M.C. (2015) The pure rotational spectrum of thorium monosulfide, ThS. *Chemical Physics Letters*, **639**, 304–306.)

molecular beam can be excited at two different locations. Most of the power is in the laser beam that is first to intersect the molecular beam. This is used to deplete the population of the rotational state (J) from which excitation occurs. Some distance downstream, the weaker component of the laser beam is used to excite the same rotational line, and the intensity of the fluorescence from this second excitation is monitored. Between the two laser beams, the molecular beam is excited by microwave radiation. When this is resonant with the $J - 1 \rightarrow J$ transition, the population transfer increases the LIF signal. By this means, Steimle et al. [89] were able to record pure rotational transitions for ThS ranging from $J = 7$ to $J = 14$, with a linewidth of 25 kHz. Previous attempts to record the ThS microwave spectrum by using the one-photon excitation techniques that yielded spectra for ThO were unsuccessful. The dipole moment of ThS [82] is slightly larger than that of ThO [81], so it seems that the problem was the production of ThS by laser ablation. We have found that it is easier to make actinide oxides and fluorides with laser ablation, as compared to other chalcogenides or the heavier halogens. The high sensitivity of the MODR method compensates for the low chemical yield, permitting microwave studies of species that are more challenging for gas-phase production.

Resonantly enhanced two-photon ionization techniques have proved to be particularly useful for studies of actinide-containing molecules [7–9]. These methods have the advantage that they can be combined with the mass-resolved detection of ions. In many cases, this mass filter can extract the spectrum for a single species from a complex chemical environment. It can also be used to separate spectra of isotopes, where small isotopic shifts result in congested LIF spectra. Note also that methods that utilize charged particle detection can be far more sensitive than those based on fluorescence detection [79].

The apparatus shown in Figure 1.3 is a typical setup for the recording of mass-resolved, resonantly enhanced multiphoton ionization (REMPI) spectra. The supersonic jet from a laser ablation source is skimmed into the second differentially pumped vacuum chamber (right-hand side of Figure 1.3), forming a well-defined molecular beam. The second chamber houses the components of a Wiley-McLaren time-of-flight mass spectrometer (TOF-MS). Two overlapping pulsed laser beams traverse the molecular beam near the center of the TOF-MS. The lasers have pulse durations of approximately 10 ns, and their synchronization is controlled by a precision pulse delay generator. The ions produced by photoionization are deflected into the flight tube by voltages applied to the repeller and draw-out grids. They are detected by microchannel plates. With a flight path of 40 cm, this system achieves near-unit-mass resolution for masses near 250 amu.

With sequential excitation, there are two options for recording REMPI spectra. In the first scheme, the first laser excites the molecule via a resonant transition. The second laser operates at a fixed photon energy that is high enough to ionize the excited molecules, but not sufficient to ionize from the ground state. The wavelength of the first laser is scanned, and the ion of interest is monitored using the mass spectrometer. It is, of course, straightforward to record the spectra associated with every observed mass peak independently, in a single spectral sweep. The data obtained are equivalent to the absorption spectra for the neutral molecules.

Conversely, the first laser can be fixed on a resonant transition and the second laser scanned in order to locate the ionization threshold (the plot of ion current versus photon energy is often referred to as a photoionization efficiency (PIE) curve).

This measurement can provide a reasonably accurate ionization energy, with uncertainties on the order of $\pm 30\,cm^{-1}$ (± 4 meV). The choice of the first laser resonance can be used to ensure that the signal is exclusively associated with ground state molecules (often a particular rotational level of the zero-point level). Tuning the second laser above the ionization limit can result in a very structured spectrum. The structure is due to the presence of strong auto-ionizing resonances that are embedded in the ionization continuum. The resonances are members of Rydberg series that converge to the rovibronic states of the molecular ion. The high-*n* Rydberg states that exist just beneath each threshold for producing the ion in a particular *v, J* state are unusually long-lived. This property can be exploited in order to obtain spectroscopic data for the molecular ion, using a technique known as pulsed-field ionization zero electron kinetic energy (PFI-ZEKE) spectroscopy [90–92]. In this experiment, a pulsed laser is used to excite the molecule to a small group of high-*n* Rydberg states under field-free conditions. For final ion states that lie above the ionization threshold (e.g., MX^+ $v = 1$), the laser pulse will also cause direct photoionization and rapid auto-ionization. Electrons that are produced by these fast processes are allowed to dissipate during a time interval of a few microseconds. A weak pulsed electric field is then applied. Molecules that are in the high-*n* Rydberg states are ionized by this pulse, and the electrons are accelerated to a microchannel plate detector. Note that PFI-ZEKE spectroscopy can be carried out using single-photon excitation, but the resolution is substantially improved if resonant two-color excitation is employed. The resolution of the two-photon technique, which is determined by the magnitude of the pulsed field, can be as low as $0.5\,cm^{-1}$. These measurements provide accurate ionization energies and well-resolved spectra for the molecular ions. Rotational resolution has been achieved for diatomic ions.

A valuable facet of the PFI-ZEKE technique is that there are few selection rules governing the ion final states can be observed. For example, Goncharov et al. [93] were able to characterize ten low-lying electronic states of UO^+, with Ω values ranging from 0.5 to 5.5. The ability to recover complete maps of low-lying states has proved to be critical for obtaining a deeper understanding of actinide bonding motifs. Such studies of UO^+ and UF^+ [31] show that the U 5*f* orbitals do not participate significantly in the bonding of these ions.

1.3.6 Anion Photodetachment Spectroscopy

Just as PFI-ZEKE spectroscopy can provide information on the low-lying states of a molecular cation, anion photodetachment spectroscopy can reveal the low-energy states of a neutral molecule [33, 94–96]. An advantage of working with anions is that the species of interest can be mass-selected prior to laser excitation. The study of small metal clusters illustrates problems that can be circumvented by working with anions. Previously we have attempted to record spectra for Th_n and U_n with n = 2 or 3 using the mass-resolved REMPI method, in the hope of probing actinide metal–metal bonds. The target ions were readily observed, but their visible range excitation spectra did not exhibit a resolvable structure. Larger metal clusters were present in the laser ablation plume, and it is most probable that these clusters suffered facile multiphoton fragmentation processes. This caused the effectively featureless spectra of the larger clusters to contribute to the signal from the M_2^+ and M_3^+ ions. This problem can be averted when mass selection can be applied prior to laser excitation.

Anion photodetachment measurements use a fixed wavelength laser for detachment. The ejected electrons have kinetic energies (eKE) that are determined by the expression

$$eKE = h\upsilon - EA - E_{Int} \tag{1.1}$$

where hυ is the photon energy, EA is the electron affinity of the neutral molecule, and E_{Int} is the internal energy of the neutral molecule (this model assumes that the anions are cooled to a low internal temperature prior to photodetachment). Hence, the electron kinetic energy distribution encodes the internal energy states of the molecule. A variety of methods have been used to measure the electron kinetic energy distributions. This proves to be a technically challenging problem that is usually the step that limits the resolution. Prior to the development of electron imaging methods, magnetic bottle spectrometers were state of the art, achieving resolutions on the order of 5–10 meV (40–80 cm^{-1}). A considerable improvement in resolution, down to a few cm^{-1}, has been realized by using velocity-map imaging techniques to characterize the detached electrons [94, 95]. With this method, an electrostatic lens is used to project the photodetached electrons along the axis of a flight tube, and image them on a position-sensitive detector (MCPs combined with a phosphor screen and a digital camera). To facilitate the description of this method, Figure 1.9 shows the velocity-map imaging spectrometer used by Wang and coworkers [95].

The components on the left-hand side of this diagram (up to the valve labeled GV2) are used for generation of the anions by laser ablation, followed by time-of-flight mass selection of the target anion. The components for velocity-map imaging (VMI) are housed in the final chamber on the right-hand side of the figure. To understand the images that this instrument produces, consider a photodetachment process that ejects electrons without a preferred direction (isotropic angular distribution). The electrons associated with a specific final state of the molecule will have a fixed velocity, and their

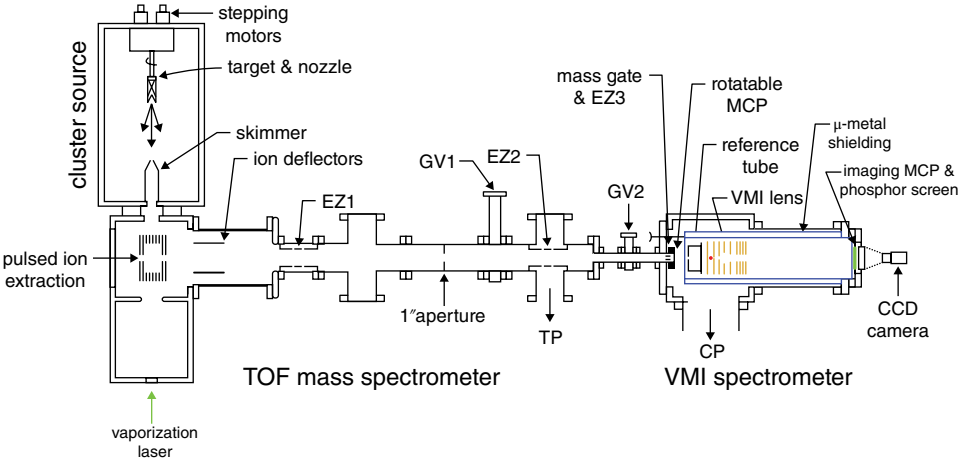

Figure 1.9 Overall schematic view of the high-resolution photoelectron spectroscopy apparatus for size-selected clusters using velocity-map imaging (VMI). (Reproduced with permission from Leon, I., Yang, Z., Liu, H.-T., and Wang, L.-S. (2014) The design and construction of a high-resolution velocity-map imaging apparatus for photoelectron spectroscopy studies of size-selected clusters. *Review of Scientific Instruments*, **85**, 083106/1–083106/12.)